HHS Public Access

Author manuscript

Nat Immunol. Author manuscript; available in PMC 2013 December 01.

Published in final edited form as:

Nat Immunol. 2013 June ; 14(6): 584–592. doi:10.1038/ni.2585.

IL-17-committed Vγ4+ γδ T cell deficiency in a spontaneous Sox13 mutant CD45.1 congenic mouse substrain protects from dermatitis

Elizabeth E. Gray[1,2,3], **Francisco Ramírez-Valle**[1,2,4], **Ying Xu**[1,2], **Shuang Wu**[1,2], **Zhihao Wu**[5], **Klaus E. Karjalainen**[5], and **Jason G. Cyster**[1,2,*]

[1]Howard Hughes Medical Institute, University of California San Francisco (UCSF), California, USA

[2]Department of Microbiology and Immunology, University of California San Francisco (UCSF), California, USA

[3]Biomedical Sciences Graduate Program, University of California San Francisco (UCSF), California, USA

[4]Department of Dermatology, University of California San Francisco (UCSF), California, USA

[5]School of Biological Sciences, Nanyang Technological University, Singapore

Abstract

IL-17-committed γδ T (γδT17) cells participate in many immune responses but their developmental requirements and subset specific functions remain poorly understood. Here we report that a commonly used CD45.1+ congenic C57BL/6 mouse substrain is characterized by a selective deficiency in Vγ4+ γδT17 cells. This trait is due to a spontaneous mutation in the transcription factor *Sox13* that causes an intrinsic defect in development of these cells in the neonatal thymus. γδT17 cells migrate at low rates from skin to lymph nodes. In a model of psoriasis-like dermatitis, Vγ4+ γδT17 cells expand markedly in lymph nodes and home to inflamed skin. Sox13 mutant mice are protected from psoriasis-like skin changes, identifying a role for Sox13-dependent γδT17 cells in this inflammatory condition.

Recent work has shown that γδ T cells are an important source of interleukin 17 (IL-17) during a variety of infections and autoimmune diseases[1–8]. These “innate-like” IL-17-committed γδ T (γδT17) cells are present in lymph nodes (LNs) as well as peripheral tissues including the dermis, lung and peritoneal cavity. γδT17 cells express many of the hallmarks

*Correspondence should be addressed to J.G.C. (jason.cyster@ucsf.edu); Phone 415 502-6427; Fax 415 502-8424.

ACCESSION CODES

Primary accession

Sequence Read Archive #

AUTHOR CONTRIBUTIONS

E.E.G., F.R.V. and J.G.C. designed the experiments; E.E.G. did most of the experiments; F.R.V. and E.E.G. did the psoriasis experiments; Y.X. and S.W. did the gene-expression analysis; Z.W. and K.E.K. provided the anti-SCART2 antibody; E.E.G., F.R.V. and J.G.C. analyzed the data; and E.E.G. and J.G.C. wrote the paper.

of T_H17 αβ T cells, including CCR6, RORγt and IL-23R[2, 9]. However, unlike T_H17 cells, γδT17 cells differentiate into IL-17-commited cells in the thymus and emerge as effector cells capable of producing IL-17 rapidly following TCR stimulation and/or exposure to IL-1β and IL-23[2, 9]. γδT17 cells consist of $V\gamma4^+$ and $V\gamma6^+$ subsets[10]. $V\gamma6^+$ γδT17 cells express the invariant TCR Vγ6Vδ1 and develop in the late embryonic thymus, subsequent to Vγ5Vδ1-expressing dendritic epidermal γδ T cell (DETC) precursors[11, 12]. $V\gamma4^+$ γδT17 cells are characterized by a more diverse TCR repertoire and expression of the scavenger receptor SCART2[13]. It was suggested that these cells develop predominantly in a late embryonic time window[14]. Whether $V\gamma4^+$ and $V\gamma6^+$ subsets of γδT17 cells have distinct functions has been unclear.

Despite the increasing evidence that γδ T cells participate in multiple diseases, understanding of the factors controlling their development lags behind that of αβ T cells. The sry-related high mobility group (HMG) box family transcription factor Sox13 is enriched in developing γδ T cells and has been suggested to play a general role in γδ T cell differentiation[15]. Transgenic mice over-expressing Sox13 are characterized by a marked reduction in αβ T-lineage committed CD4 and CD8 double positive (DP) thymocytes, while γδ T cell development remains normal[15]. In contrast, embryonic day (E) 18.5 mice carrying a targeted deletion of *Sox13* are characterized by a modest (3×) reduction in the total number of γδ thymocytes[15]. These Sox13-deficient mice were reported to have severe post-natal growth abnormalities[15] precluding study of how Sox13 deficiency affects γδ T cell subsets in adult mice. More recently, Sox13 was shown to be enriched in developing γδT17 cells, though whether Sox13 is required *in vivo* for their generation or function has not been reported[16, 17].

The dynamics of γδ T cell trafficking in peripheral tissues are also poorly characterized compared to that of αβ T cells. γδT17 cells are present in both the dermis and in skin draining LNs but it has been unclear whether the dermal cells traffic to LNs. It is also not known whether, following activation in LNs, γδT17 cells are able to home to sites of inflammation.

Here we report that the $V\gamma4^+$ subset of γδT17 cells matures in the neonatal thymus in a Sox13-dependent manner. Sox13-mutant mice were protected from psoriasis-like dermatitis, implicating $V\gamma4^+$ γδT17 cells in this inflammatory skin condition. Our findings also show that γδT17 cells migrate from inflamed skin to draining LNs, undergo marked expansion in responding LNs, and home from LNs back to skin. We suggest that recirculation of expanded γδT17 cells may contribute to the systemic exacerbations in psoriasis that can occur following local imiquimod application in humans.

RESULTS

B6.SJL/NCI and B6.SJL/Tac mice lack $V\gamma4^+$ γδT17 cells

During experiments with $CD45.2^+$ C57BL/6N (B6/NCI) and congenic $CD45.1^+$ (B6.SJL/NCI) strains from NCI, we observed that $V\gamma4^+CCR6^+$ γδ T cells were severely diminished in LN cell suspensions from B6.SJL/NCI mice (Fig. 1a,b). $CCR6^+$ γδ T cells correspond to a population of IL-17-committed γδ T (γδT17) cells[18]. Consistent with the lack of

Vγ4$^+$CCR6$^+$ γδT17 cells in B6.SJL/NCI mice, the number of LN Vγ4$^+$ γδ T cells expressing IL-17A following phorbol ester plus ionomycin (PMA+I) stimulation was markedly reduced (Fig. 1c,d). On the other hand, the number of LN Vγ4$^-$ γδ T cells, αβ T cells and non-T cells expressing IL-17A was similar in both strains (Fig. 1c,d).

Consistent with a recent report[13], LN Vγ4$^+$, but not Vγ4$^-$, CCR6$^+$ γδT17 cells expressed the scavenger receptor SCART2 (Supplementary Fig. 1a). SCART2 was also expressed by a subset of LN IL-7Rα^{hi}CCR6$^+$ non-γδT cells, a population that is also IL-17-committed[19, 20] (Supplementary Fig. 1c). Vγ4$^+$SCART2$^+$CCR6$^+$ γδT17 cells were nearly absent in LNs from B6.SJL/NCI mice, whereas the frequency of SCART2$^+$IL-7Rα^{hi}CCR6$^+$ non-γδ T cells was unchanged (Supplementary Fig. 1a,c,e).

SCART2 expression by dermal TCRγδ^{int} cells was also reported[13]; we found it stains the Vγ4$^+$CCR6$^+$ subset (Supplementary Fig. 1b). Vγ4 staining by CCR6$^+$TCRγδ^{int} cells was weak when we used dispase digestion to separate epidermal and dermal ear skin sheets (Supplementary Fig. 1b), suggesting the Vγ4 epitope is sensitive to dispase. Therefore, we used SCART2 to define Vγ4$^+$ γδT17 cells in dispase-prepared dermal cell suspensions, while Vγ4$^+$ staining was used in whole ear skin cell suspensions prepared without dispase. Consistent with observations in the LN, we observed severely diminished numbers of SCART2$^+$CCR6$^+$ γδT17 cells in dermal cell suspensions, while SCART2$^-$CCR6$^+$ γδT17 cells (Fig. 1d and Supplementary Fig. 1b) and SCART2$^+$IL-7Rα^{hi}CCR6$^+$ non-γδ T cells (Supplementary Fig. 1d,f) were unchanged. We observed a similar lack of Vγ4$^+$CCR6$^+$ γδT17 cells in the spleen, peritoneal cavity and lung, while CCR6$^-$ γδ T cells were present at normal frequencies (Supplementary Fig. 2a–d). Together, these data suggest that production of SCART2$^+$Vγ4$^+$ γδT17 cells is specifically impaired in B6.SJL/NCI mice.

To explore the nature of this defect, we asked whether Vγ4$^+$ γδT17 cells were present in other substrains. Edward Boyse generated CD45.1$^+$ congenic C57BL/6 mice by backcrossing the CD45.1 allele expressed by SJL mice onto the C57BL/6 background[21]. The National Cancer Institute (NCI) as well as Jackson Laboratory (Jax), Taconic Farms (Tac) and Charles River Laboratories (CR) maintain colonies of this strain, which we refer to as “B6.SJL/Vendor”. Vγ4$^+$CCR6$^+$ γδT17 cells were present at normal frequencies in SJL mice, suggesting that genetic polymorphisms in SJL mice were unlikely to contribute to the defect in B6.SJL/NCI mice (Fig. 1f). The B6.SJL strain maintained at NCI was imported from the Boyse laboratory to the Mathieson laboratory at the NIH in the 1970s, and transferred to NCI in the 1980s. Tac received this strain from NCI in 1995 and refreshed their colony from NCI stock in 2007. Jax imported this strain from the Boyse laboratory in 1990; CR USA received this strain from CR France in 2010. Like B6.SJL/NCI mice, B6.SJL/Tac mice were characterized by Vγ4$^+$CCR6$^+$ γδT17 cell deficiency, while frequencies were normal in B6.SJL/Jax and B6.SJL/CR mice (Fig. 1f). These data suggest that a spontaneous mutation became fixed in the B6.SJL/NCI colony prior to 2007 (when Tac refreshed their colony from NCI stock).

Loss of Vγ4$^+$ γδT17 cells is due to a spontaneous Sox13 mutation

When B6/NCI and B6.SJL/NCI mice were intercrossed, F_1 offspring had normal frequencies of LN Vγ4$^+$CCR6$^+$ γδT17 cells, suggesting the B6.SJL/NCI trait was recessive. Analysis of

121 F_2 offspring obtained by intercrossing the F_1 mice revealed that 94 (~78%) mice had normal frequencies, while 27 (~22%) mice had diminished frequencies of LN $V\gamma4^+CCR6^+$ γδT17 cells (Fig. 2a). Moreover, the B6.SJL/NCI trait was tightly linked to the *Ptprc* locus, although genetic complementation with CD45-deficient mice suggested the mutation was not in *Ptprc* itself (Fig. 2b,c). Based on 27 F_2 mice (54 meioses, 3 recombination events, Fig. 2c) and additional analysis of 95 offspring from F_1 mice backcrossed to B6.SJL/NCI mice (95 meioses, no recombination events), we calculated a linkage distance of 2 cM (3/149). These data suggested the B6.SJL/NCI trait was controlled by a single locus located within approximately 2 cM of *Ptprc*

Whole exome sequencing of B6.SJL/NCI mouse DNA and comparison to the reference B6 genome sequence identified 86 non-synonymous coding variants in genes located within 3 cM of *Ptprc*. We ruled out 84 of these variants as they were present in mouse strains that have $V\gamma4^+CCR6^+$ γδT17 cells (Supplementary Figs. 3a, b and Supplementary Tables 1 and 2). One coding variant was not confirmed by Sanger sequencing and was excluded. The one coding variant remaining (Supplementary Table 2) was a single C nucleotide insertion at codon 330 in *Sox13* (c.987_988insC, Ensembl transcript ID: ENSMUST00000094551) that resulted in a premature stop codon 9 amino acids downstream (p.S330QfsX9) (Fig. 3a,b). The stop codon was upstream of the DNA-binding HMG domain, but downstream of the leucine zipper and glutamine-rich region[22, 23]. We confirmed by Sanger sequencing that this mutation was present in B6.SJL/NCI and B6.SJL/Tac mice, but absent from B6.SJL/Jax and B6.SJL/CR mice.

To explore whether the mutation affected *Sox13* mRNA abundance, we sorted $V\gamma4^+$ and $V\gamma4^-CD24^{hi}$ γδ thymocytes and measured *Sox13* transcripts by real-time PCR using primers spanning exons 1–2, 6–7 and 12–13. *Sox13* transcripts were more abundant in wild-type $V\gamma4^+CD24^{hi}$ than $V\gamma4^-CD24^{hi}$ γδ T thymocytes (Fig. 3c), consistent with previous data[17]. Importantly, *Sox13* transcripts were diminished ~7 fold in $V\gamma4^+CD24^{hi}$ γδ T cells in B6.SJL/NCI mice (Fig. 3c), likely due to the premature stop codon inducing nonsense-mediated decay[24]. Thus, B6.SJL/NCI mice harbor a spontaneous *Sox13* mutation that introduces a stop codon in the middle of the open reading frame; we refer to this disrupted allele as $Sox13^{mut}$.

Sox13 intrinsically regulates development of $V\gamma4^+$ γδT17 cells

Next, we tested whether the defect in $Sox13^{mut/mut}$ (B6.SJL/NCI) mice was intrinsic to hematopoietic cells. γδT17 cells are produced in an early wave in the embryonic and neonatal thymus and are poorly reconstituted by bone marrow (BM) transferred into irradiated wild-type mice[14, 19, 25]. In previous work we also saw poor reconstitution of γδT17 cells by BM in irradiated TCRδ-deficient recipients unless we co-transferred neonatal thymocytes[19]. Here, while we continued to find that neonatal thymocytes gave the most efficient reconstitution (not shown), transfer of wild-type BM to irradiated TCRδ-deficient mice was sufficient to reconstitute $V\gamma4^+CCR6^+$ γδT17 cells when we waited at least 12 weeks (Fig. 4a,b). The basis for the difference in reconstitution efficiency between studies is unclear. Importantly, however, BM from $Sox13^{mut/mut}$ mice failed to reconstitute $V\gamma4^+CCR6^+$ γδT17 cells in irradiated TCRδ-deficient hosts (Fig. 4a,b).

LN CCR6^{-} γδ T cells, which are not IL-17-committed and include predominantly Vγ4^{+} and Vγ1^{+} cell subsets (Supplementary Fig. 4a,b), are efficiently reconstituted by BM transfer[14] and reconstitution was unaffected by the *Sox13* mutation (Fig. 4a,b). In contrast, Vγ4^{-}CCR6^{+} γδT17 cells, which are predominantly Vγ6^{+} cells (Supplementary Fig. 4a,b)[3, 9, 14] that develop in the late embryonic period[11, 12], were not reconstituted by BM transplantation (Fig. 4a,b). This may reflect a strong requirement for the embryonic thymus for Vγ6^{+} γδT17 cell development[14].

We also examined the corresponding cells in the ear skin dermis, using SCART2 to identify the Vγ4^{+} subset of γδT17 cells. We observed reconstitution of SCART2^{+}CCR6^{+} γδT17 cells following transfer of BM cells from wild-type but not *Sox13*$^{mut/mut}$ mice (Fig. 4b). SCART2^{-}CCR6^{+} γδT17 cells were not reconstituted by either BM source (data not shown), consistent with the LN data.

To test whether the defect in *Sox13*$^{mut/mut}$ mice was γδT17 cell intrinsic, irradiated TCRδ-deficient mice were reconstituted with a mixture of CD45.2^{+} wild-type and CD45.1^{+} wild-type or *Sox13*$^{mut/mut}$ BM. While Vγ4^{+}CCR6^{-} γδ T cells were reconstituted in this mixed setting by BM from both sources, *Sox13*$^{mut/mut}$ BM failed to reconstitute LN Vγ4^{+}CCR6^{+} and dermal SCART2^{+}CCR6^{+} γδT17 cells (Fig. 4c). Together, these data suggest that a cell intrinsic defect in *Sox13*$^{mut/mut}$ mice selectively blocks the development of Vγ4^{+} γδT17 cells.

Impaired maturation of Vγ4^{+} γδT17 cells in the neonatal thymus

Given that *Sox13*$^{mut/mut}$ (B6.SJL/NCI) mice lack Vγ4^{+}CCR6^{+} γδT17 cells in all tissues examined, we asked whether their development in the neonatal thymus[19, 26] was blocked. Analysis of *Sox13*$^{mut/mut}$ neonates at day 0 post-birth revealed Vγ4^{+} γδT17 cells that were CD24^{hi}CCR6^{neg}, indicating an immature phenotype (Fig. 5a). At day 5, a greater number of Vγ4^{+} γδT17 cells were present and approximately 20–30% had a mature CD24^{low}CCR6^{+} phenotype (Fig. 5a). In *Sox13*$^{mut/mut}$ neonates, Vγ4^{+} γδT17 cells were numerically reduced and they failed to reach a CD24^{low}CCR6^{+} phenotype (Fig. 5a,b), suggesting their maturation was blocked.

In contrast, Vγ4^{-} γδT17 cells were more abundant and many had a mature CCR6^{+}CD24^{lo} phenotype in neonates at day 0; by day 5, nearly all were CCR6^{+}CD24^{lo} mature cells (Fig. 5c). Consistent with normal numbers of Vγ4^{-} γδT17 cells in the periphery (Fig. 1), the number of Vγ4^{-} γδT17 thymocytes in *Sox13*$^{mut/mut}$ neonates was only slightly reduced (Fig. 5d) and their maturation into CCR6^{+}CD24^{lo} cells remained intact. *Sox13*$^{mut/mut}$ Vγ4^{-} γδT17 cells also expressed normal amounts of IL-7Rα, which is abundant on γδT17 cells[19, 27] (Supplementary Fig. 5a). However, TCR surface levels on Vγ4^{-} γδT17 cells were diminished ~30%, while levels on CCR6^{-} γδ T cells were unaltered (Supplementary Fig. 5b,c). These data suggest that Vγ4^{-} γδT17 cells develop prior to Vγ4^{+} γδT17 cells and are less dependent on Sox13 for their development.

B6.SJL/NCI mice are protected from psoriasis-like dermatitis

Dermal γδT17 cells have been suggested to promote psoriasis-like dermatitis[4–6]. We asked whether *Sox13*$^{mut/mut}$ (B6.SJL/NCI) mice, which selectively lack Vγ4^{+} γδT17 cells, are protected from psoriasis-like changes. Daily application of 5% imiquimod cream to the ear skin of wild-type mice led to increased ear thickness that was reduced nearly two fold in *Sox13*$^{mut/mut}$ mice at day 5 (Fig. 6a). Histological analysis of wild-type ear skin at day 5 revealed the expected[28] epidermal thickening (acanthosis) and collections of neutrophils in the epidermis (Fig. 6b). In contrast, ear skin from *Sox13*$^{mut/mut}$ mice exhibited reduced acanthosis and fewer epidermal neutrophil pustules (Fig. 6b). Moreover, flow cytometric analysis revealed a reduction in Ly6G^{+}CD11b^{+} neutrophils in *Sox13*$^{mut/mut}$ compared to wild-type ear skin at day 3 and a trend towards fewer neutrophils at day 5 (Fig. 6c).

To assess IL-17 production by dermal cells *ex vivo*, we digested whole ear skin in the presence of Brefeldin A and stained cell suspensions for intracellular cytokine. Very little IL-17A was observed in untreated wild-type ear skin; however, after 3 days of imiquimod treatment, Vγ4^{+} and Vγ4^{-} TCRγδ^{int} cells produced IL-17A (Fig. 6e). We observed diminished IL-17 production by Vγ4^{-}TCRγδ^{int} cells from 3 day imiquimod treated *Sox13*$^{mut/mut}$ ear skin suggesting that, in addition to Vγ4^{+} γδT17 cell deficiency, Vγ4^{-} γδT17 cell function may not be fully intact (Fig. 6e). Consistent with a reduction in IL-17A production in *Sox13*$^{mut/mut}$ mice, transcripts encoding IL-17A, IL-17F, and IL-17A-targets, including the anti-microbial peptides β-defensin 3 and 4 as well as the neutrophil chemoattractant CXCL2 were reduced after 3 days of imiquimod treatment (Fig. 6d). Moreover, we observed reduced migration of Ly6G^{+}CD11b^{+} neutrophils to ear skin extracts prepared from *Sox13*$^{mut/mut}$ compared to wild-type mice harvested after 3 days of imiquimod treatment (Fig. 6f). These findings suggest that cytokine production by skin resident Vγ4^{+} γδT17 cells contributes to the magnitude of skin inflammation in the early phases of imiquimod-induced psoriasis-like dermatitis.

Dermal γδT17 cells migrate from skin to draining LNs

γδT17 cells are present in both the dermis and skin-draining LNs, although whether dermal γδT17 cells migrate to draining LNs has not been assessed. We utilized transgenic mice expressing the green-to-red photoconvertible KikGR protein[29] to track migration of cells. Similar to findings in Kaede mice[30], exposure of ear skin for 10 minutes to 415-nm violet light was sufficient to convert ear skin cells from green to red (Fig. 7a). Photoconversion was specific to ear skin cells as few KikGR-red^{+} cells were detected in the draining LN or blood immediately after photoconversion (Supplementary Fig. 6a). Violet light exposure did not lead to measurable inflammation as assessed by induction of IL-1β transcripts (Supplementary Fig. 6b), consistent with earlier findings[30–32]. Analysis of draining cervical LNs 24 hours later showed that 1–5% of CCR6^{+} γδT17 cells were KikGR-red^{+}, suggesting that dermal γδT17 cells migrate to draining LNs at a low rate in the steady-state (Fig. 7b). A similar fraction of LN MHCII^{hi}CD11c^{+} dendritic cells were KikGR-red^{+} (Supplementary Fig. 6c)[30, 32]. We next treated ear skin with imiquimod or control cream daily for 1, 3, or 5 days and photoconverted the ear skin 24 hours prior to analysis. The number of KikGR-red^{+} CCR6^{+} γδT17 cells in the draining LNs was unchanged at days 1 and 3, but increased slightly at day 5; this change was accompanied by a marked (~10-fold) increase in the

number of KikGR-red$^+$ CCR6$^-$ γδ T cells at day 5 (Fig. 7c,d). These CCR6$^-$ γδ T cells may correspond to activated γδT17 cells that have downregulated CCR6 expression ([33] and data not shown). As expected, we also observed an increase in the number of KikGR-red$^+$ dendritic cells in draining LNs of imiquimod-treated mice at days 3 and 5 (Supplementary Fig. 6d). These findings establish that there is an increased flux of γδ T cells from skin to draining LNs following imiquimod treatment.

Vγ4$^+$ γδT17 cells expand in LNs and home to inflamed skin

Analysis of draining LNs in wild-type mice after 5 days of imiquimod treatment revealed a marked and selective expansion of Vγ4$^+$ γδT17 cells (Fig. 8a,b), many of which were CCR6^{lo} or CCR6$^-$ (data not shown). In the blood, the number of Vγ4$^+$ γδT17 cells was also elevated (Fig. 8c). No expansion of Vγ4$^+$ γδT17 cells occurred in *Sox13*$^{mut/mut}$ mice (Fig. 8a,b). The Vγ4$^-$ subset of γδT17 cells expanded modestly and only in proportion to the increased cellularity of the draining LNs (Fig. 8a,b). Interestingly, the increase in LN Vγ4$^+$ γδT17 cells was specific to cells expressing Vδ4 (Fig. 8d). In the ear skin, we observed a marked increase in Vγ4$^+$Vδ4$^+$ γδT17 cells two days later, at day 7 of imiquimod treatment (Fig. 8d).

To test whether the expanded LN Vγ4$^+$ γδT17 cells had the capacity to migrate to inflamed skin, draining LN cells from wild-type CD45.2$^+$ mice harvested after 5 or 7 days of imiquimod treatment were intravenously transferred to *Sox13*$^{mut/mut}$ CD45.1$^+$ recipients that had been imiquimod treated for two days. Three hours after transfer, the ear skin, draining LNs and blood were harvested for analysis of CD45.2$^+$ cells. Compared to their frequency (~1%) in the donor population, we observed a marked enrichment for Vγ4$^+$ γδ T cells in inflamed ear skin, where they constituted ~25% of donor-derived cells, while their frequency in blood and draining cervical LNs (<2%) was similar to the input (Fig. 8e).

Given the ability of Vγ4$^+$ γδT17 cells to efficiently home to inflamed skin, we asked whether psoriasis-like changes could be promoted by transferring LN cells from day 5 imiquimod-treated wild-type mice. We transferred 30–50 million total LN cells into *Sox13*$^{mut/mut}$ recipients that had been treated for 1 day with imiquimod and analyzed the recipients 2 days later. Donor Vγ4$^+$ γδ T cells accumulated in the treated ear skin at frequencies even greater than observed 3 hours after transfer (Fig. 8e,f). While the percentage of donor-derived cells corresponding to Vγ4$^+$ γδ T cells in the blood and draining LNs was low (less than 3%), Vγ4$^+$ γδ T cells constituted the majority (66–85%) of donor-derived cells in the ear skin (Fig. 8f). Moreover, nearly all IL-17$^+$ donor-derived cells in the ear skin were Vγ4$^+$ γδT17 cells, suggesting that, among donor IL-17-committed cells, Vγ4$^+$ γδT17 cells selectively accumulated in inflamed skin (Fig. 8f). The reason for increased frequencies of donor Vγ4$^+$ γδT17 cells in inflamed skin harvested at 2 days compared to 3 hours after transfer could be due to continued homing from blood and expansion or enhanced survival of the cells. Importantly, there was more than a two-fold increase in the frequency of neutrophils in ear skin of *Sox13*$^{mut/mut}$ mice receiving wild-type cells compared to no donor cells (Fig. 8g). Transcripts encoding IL-17A and IL-17F, and the IL-17A-targets CXCL2 and β-defensin 3, were elevated in wild-type cell recipients (Fig. 8h). The selective accumulation of Vγ4$^+$ γδT17 cells among IL-17-committed cells favors the view that

Sox13-dependent Vγ4$^+$ γδT17 cells promote dermatitis, although we cannot rule out potential contributions from other donor LN cells. Together, these data are consistent with a model in which Vγ4$^+$ γδT17 cells expand in the draining LN, recirculate to inflamed skin and promote IL-17-driven inflammatory changes.

DISCUSSION

Here we describe a selective deficiency for Vγ4$^+$ γδT17 cells in the NCI and Taconic substrains of CD45.1$^+$ congenic C57BL/6 mice due to a spontaneous mutation in the transcription factor *Sox13*. We show that Sox13-dependent cells, most likely Vγ4$^+$ γδT17 cells, contribute to psoriasis-like dermatitis as IL-17 pathway activity and skin inflammation are reduced in *Sox13*$^{mut/mut}$ skin. Moreover, Vγ4$^+$ γδT17 cells undergo marked expansion in draining LNs and home to inflamed skin where they promote inflammatory changes. While our identification of a spontaneous *Sox13* mutation in two widely used substrains establishes a need for caution in interpreting IL-17 responses in these mice, the ready availability of *Sox13*$^{mut/mut}$ mice should facilitate analysis of γδT17 cell contributions to a range of immune responses. In addition to psoriasis-like dermatitis, γδT17 cells have been implicated in autoimmune encephalomyelitis,[1, 2] collagen-induced arthritis[3], and a variety of bacterial infections[1, 7, 8]. We anticipate that cytokine production by resident Vγ4$^+$ γδT17 cells, as well as their expansion, recirculation and tissue-specific homing will be involved in many of these responses.

Sox13 is upregulated early during γδ T cell development and, based on studies in *Sox13*$^{-/-}$ embryonic mice, was suggested to promote γδ T-lineage commitment[15, 17]. Our analysis of adult *Sox13*$^{mut/mut}$ mice, which have normal frequencies of CCR6$^-$ γδ T cells, suggests Sox13 may not be essential for γδ T lineage commitment. Accordingly, recent studies have shown that some developing γδ T cell subsets express little Sox13[16, 34, 35]. However, the *Sox13* frameshift mutation may not completely inactivate Sox13, and we therefore cannot exclude the possibility that residual activity of a splice variant or truncated protein sustains development of some Sox13-dependent cells. In contrast to *Sox13*$^{mut/mut}$ mice, *Sox13*$^{-/-}$ mice suffer severe postnatal growth defects[15]. The basis for the difference in postnatal viability is unclear, but could be due to residual Sox13 activity in *Sox13*$^{mut/mut}$ mice or to off-target mutations in mice derived from *Sox13*$^{-/-}$ embryonic stem cells. Future comparisons of these and further Sox13-mutant mouse lines should resolve between these possibilities.

How Sox13 promotes Vγ4$^+$ γδT17 cell development is unclear, but may involve interaction with TCF-1, an HMG transcription factor involved in αβ T cell development[15, 36]. TCF-1 represses *Il17a* and inhibits T_H17 differentiation[37, 38] suggesting Sox13 may antagonize TCF-1-mediated *Il17a* repression in γδ T cells. Moreover, recent work suggests that Sox13 may promote γδT17 cell differentiation by upregulating IL-7Rα[16]. However, these observations do not explain the more pronounced role we observed for Sox13 in Vγ4$^+$ versus Vγ4$^-$ γδT17 cell development. Further work will be needed to determine the Sox13 target genes that are essential for Vγ4$^+$ γδT17 cell development and to discern how it contributes to Vγ4$^-$ γδT17 cell maturation.

Precisely when Vγ4$^+$ γδT17 cells develop in the thymus has not been clearly defined, as γδT17 cells have been reported in the embryonic, neonatal and adult thymus[14, 16, 18, 26, 39]. Here, we found that immature Vγ4$^+$ γδT17 cells were present in the thymus at birth and subsequently matured into CD24^{lo}CCR6$^+$ cells, suggesting Vγ4$^+$ γδT17 cells develop in the early postnatal thymus. In contrast, mature CD24^{lo}CCR6$^+$Vγ4$^-$ γδT17 cells were already present in the thymus at birth, suggesting that Vγ4$^-$ γδT17 cells develop in an earlier wave. Given that γδT17 cells include predominantly Vγ4$^+$ and Vγ6$^+$ subsets[14], most Vγ4$^-$ γδT17 cells likely correspond to Vγ6$^+$ γδT17 cells, which develop primarily in the embryonic thymus subsequent to Vγ5$^+$ dendritic epidermal γδ T cell precursors[11, 12, 14, 16].

CCR6$^+$ γδT17 cells are present in the mouse dermis and are enriched in skin-draining LNs. Our findings with KikGR mice suggest that CCR6$^+$ γδT17 cells have the capacity to migrate from the skin to draining LNs in the steady state. We used violet light to photoconvert KikGR, which, in contrast to ultraviolet light, is not thought to cause inflammatory changes[30–32]. However, we cannot rule out the possibility that violet light exposure may have certain immunomodulatory effects that affect cell migration. Nonetheless, the ability of dermal γδT cells to migrate to draining LNs is consistent with the possibility that the LN population may, at least in part, be skin-derived, although some may also be maintained as a separate pool. Analysis of skin-draining lymph in cattle, a species rich in γδ T cells, demonstrates a substantial flux of γδ T cells through the skin to draining LNs[40]. Imiquimod treatment promoted an increase in γδ T cell migration from the skin to draining LNs, with many of the migrating cells being CCR6$^-$. Given that CCL20 is highly upregulated in inflamed skin[41], this raises the possibility that CCR6 downregulation promotes egress of activated γδT17 cells from the skin.

Recent studies have reported that γδT17 cells expand in the skin and draining LNs following imiquimod treatment[4, 6]. Here, we observed a selective accumulation of Vγ4$^+$Vδ4$^+$ γδT17 cells in draining LNs at day 5, likely due mostly to proliferation in the LN as many of the cells were blasting and rapidly incorporated BrdU (unpubl. obs.). Vγ4$^+$Vδ4$^+$ γδT17 cell expansion in draining LNs was also reported following subcutaneous injection of complete Freund's adjuvant[3]. What promotes Vγ4$^+$Vδ4$^+$ γδT17 cell expansion is unclear, but may include induction of both inflammatory cytokines (e.g. IL-1β and IL-23) and their cognate TCR ligand. IL-7 may also contribute as it is sufficient to promote γδT17 cell proliferation in LNs[27].

The paradigm of expansion in LNs followed by circulation and selective homing to inflamed tissue has been central to understanding αβT cell responses[42]. Our findings add to limited earlier data[3, 43] to demonstrate that γδT17 cells may also follow this paradigm as they undergo massive LN expansion and are capable of efficient homing to inflamed skin. Clinical use of topical imiquimod treatment for cutaneous pre-cancers can lead to psoriasis exacerbations, including at distal sites[44]. Recent work identified human circulating, skin-homing CLA$^+$CCR6$^+$ γδ T cells that can be recruited to perturbed skin and are increased in psoriasis lesions[45]. Thus, it is tempting to speculate that local imiquimod treatment in humans may promote expansion and recirculation of activated, skin-homing IL-17-committed lymphocytes that are then available for recruitment to distal skin sites.

METHODS

Mice

C57BL/6 mice were purchased from the National Cancer Institute (NCI, 01C55, C57BL/6NCr), Jackson Laboratory (Jax, 000664, C57BL/6J), Taconic Farms (Tac, B6, C57BL/6NTac), and Charles River Laboratories (CR, 027, C57BL/6N). CD45.1$^+$ congenic mice were from NCI (01B96, B6-LY5.2/Cr), Jax (002014, B6.SJL-*Ptprc*^{a}*Pepc*^{b}/BoyJ), Tac (4007, B6.SJL-*Ptprc*^{a}/BoyAiTac), and CR (494, B6.SJL-*Ptprc*^{a}*Pepc*^{b}/BoyCrl). Unless otherwise indicated, data shown are from C57BL/6N and B6-LY5.2/Cr mice from NCI. FVB/N mice were provided by Dr. L. Coussens. *Ptprc*$^{-/-}$ mice[46] were provided by Dr. A. Weiss. A/J (000646), DBA/2 (000671), PWD (004660), *Tcr*δ$^{-/-}$ (002120) and *CAG::KikGR*$^{Tg/+}$ (013753)[29] mice were from Jax. NOD mice were provided by Dr. Q.Tang or Jax (001976). *CAG::KikGR*$^{Tg/+}$ mice were on a mixed C57BL/6 and outbred ICR background and backcrossed to C57BL/6 for 2–4 generations. All experiments were approved by the UCSF Institutional Animal Care and Use Committee.

Tissue preparation

Lymph nodes (LN) and ear skin were digested as described[19]. Briefly, LN and minced lungs were digested with 67μg/ml Liberase TM (Roche Applied Science) and 20μg/ml DNAseI (Sigma) for 20–30 minutes at 37°C while rotating. Ears were split into dorsal and ventral halves and digested in 2mg/ml Dispase (Gibco). Separated epidermal and dermal sheets were digested in DMEM containing penicillin/streptomycin, HEPES buffer, 85μg/ml Liberase TM (Roche Applied Science), 100μg/ml DNAseI (Sigma), 0.5mg/ml hyaluronidase (Sigma) and 2% fetal calf serum at 37°C for 60–120 minutes while rotating. Alternatively, whole ear skin was minced and digested with Liberase, DNAseI, and hyaluronidase as described above. Digestion enzymes were quenched by the addition of 5mM EDTA and 1% serum. All tissues were disaggregated by passing through a 70μm or 100μm nylon sieve (BD Bioscience). For Vγ1 staining, LNs were not digested as the Vγ1 epitope recognized by anti-Vγ1 (clone 2.11) was found to be sensitive to digestion with Liberase TM (Roche Applied Science).

Flow cytometry

Cell suspensions were stained as previously described[47] with the following antibodies: Vγ4 (UC3-10A6), Vδ4 (GL2), Vγ1 (2.11), TCRγδ (GL3), TCRβ (H57-597), IL-17A (eBio17B7), CD196/CCR6 (140706), CD4 (clone GK1.5), CD24/HSA (M1/69), CD11b (clone Mac-1), Ly6G (clone 1A8), CD45.2 (clone 104) and CD45.1 (clone A20) (Biolegend, BD Biosciences, eBioscience, Cedarlane Laboratories, or Invitrogen). SCART2 staining was performed using anti-SCART2 polyclonal rat serum[13] followed by biotin-conjugated anti-rat IgG (Jackson Immunoresearch). All biotin-conjugates were detected with streptavidin Qdot®605 (Invitrogen). For intracellular IL-17A staining, cells were stimulated for 2 hours with 50ng/ml phorbol myristate acetate (Sigma) and 1ug/ml ionomycin (EMD Biosciences) in brefeldin A (BD Biosciences). Cells were stained with fixable viability dye (eFluor®780, eBioscience) per manufacturers instructions to exclude dead cells, blocked with anti-CD16/32 (clone 2.4G2, UCSF hybridoma core) in 5% normal mouse and rat serum, stained for surface antigens, and fixed with BD Cytofix Buffer; following permeabilization with

Perm/Wash reagent (BD Biosciences), cells were stained with anti-IL-17A (eBioscience, clone eBio17B7).

Cell Sorting

For analysis of Sox13 transcripts, thymocytes were incubated with anti-CD4 and anti-CD8 microbeads (Miltenyi Biotec) and depleted of labeled cells by autoMACS (Miltenyi Biotec) per manufacturer's instructions. Thymocytes were blocked with anti-CD16/32 (clone 2.4G2, UCSF hybridoma core) in 5% normal mouse and rat serum in DMEM/10%FBS/5μM EDTA and stained with anti-Vγ4-FITC, anti-TCRδ-PE, anti-CCR6-AlexaFluor647, and anti-CD24-biotin. The CD24-biotin conjugate was detected with streptavidin Qdot®605. Dead cells were excluded with DAPI and $V\gamma4^{+}TCR\gamma\delta^{+}CD24^{+}CCR6^{-}$ and $V\gamma4^{-}TCR\gamma\delta^{+}CD24^{+}CCR6^{-}$ thymocytes subsets were sorted on a FACSAria with a purity of at least 98%.

Real-time PCR

Total RNA was isolated and converted to cDNA as previously described[47]. Real-Time PCR was performed on a StepOnePlus™ Real-Time PCR system (Applied Biosystems) using iTaq SYBR Green Supermix (Bio-Rad) and primer pairs (Integrated DNA Technologies) listed in Supplementary Table 4.

Imiquimod model of psoriasis-like dermatitis

B6/NCI and B6.SJL/NCI mice between 6–12 weeks of age were treated daily for up to 7 days with 5mg of 5% imiquimod cream (Imiquimod Cream 5%, Fougera Pharmaceuticals Inc.) or control cream (Vanicream™, Pharmaceutical Specialties, Inc.) on each ear. In some initial experiments, mice were also treated with 50mg of 5% imiquimod cream on shaved and depilated back skin; however, as previously reported[28] for mice on a C57BL/6 background, these mice exhibited flu-like symptoms likely due to systemic effects of imiquimod. Therefore, in subsequent experiments, we treated ear skin only. Ear thickness was measured daily with digital calipers (Mitutoyo). For histological analysis, paraformaldehyde-fixed, paraffin-embedded ear skin sections were prepared and stained with hematoxylin and eosin by the UCSF Mouse Pathology Core. To identify cells that were actively producing IL-17 in ear skin, ears were digested as described above in the presence of brefeldin A (BD Biosciences). In some experiments, ears were incubated with RPMI with 10% fetal calf serum and brefeldin A for 35 minutes at 37°C prior to digestion, which increased intracellular accumulation of IL-17.

Bone marrow chimeric mice

Bone marrow cells (BM, $3–6\times10^{6}$) from B6.SJL/NCI or B6.SJL/Jax mice were transferred intravenously into *Tcr*$\delta^{-/-}$ mice lethally irradiated with a split dose of 1100–1300 rads. In some experiments, BM cells from B6.SJL/NCI or B6.SJL/Jax and B6/NCI mice were mixed. Recipient mice were analyzed at least 12 weeks later. In an earlier study, we reported that BM transplantation failed to reconstitute $CCR6^{+}$ γδ T cells in both irradiated WT and *Tcr*$\delta^{-/-}$ recipients[19]. We continue to find that BM transfers into irradiated WT recipients poorly reconstitute $CCR6^{+}$ γδ T cells, consistent with reports from multiple groups[14, 25, 48]. However, in the present experiments, transplantation of WT BM into irradiated *Tcr*$\delta^{-/-}$ mice

led to Vγ4^{+}CCR6^{+} γδ T cell reconstitution at 12 or more weeks after transfer, while reconstitution was variable at 8 weeks (data not shown). We have not determined the basis for this discrepancy in γδT17 cell reconstitution in *Tcr*δ$^{-/-}$ recipients between the past and present studies, but suggest it may reflect stringent requirements for γδT17 cell development that are not fully understood. In this regard, Haas et al. have suggested that thymic IL-17 production may negatively impact γδT17 cell reconstitution[14].

Neutrophil chemoattractant bioassay

BM cells (1×10^{6} cells) were transmigrated across 3μm transwell filters (Corning Costar) for 1.5 hours to ear skin supernatant as described[49]. Day 3 imiquimod-treated ear skin was minced and incubated while rotating for 2.5 hours at 37°C in 1.4ml of RPMI medium containing 0.5% (wt/vol) fatty acid-free BSA (two ears per 1.4ml). Ear skin suspensions were then centrifuged at 14000 rpm for 5 minutes twice and supernatant was removed. Ear skin supernatant was diluted in RPMI medium with 0.5% fatty acid-free BSA for the migration assay.

Photoconversion

A 415-nm Silver LED light source with a 1.5mm core diameter light guide and collimating adaptor (Prizmatix) was used for photoconversion. Mice were anesthetized and ventral ear skin was exposed to 415-nm violet light (~1cm diameter) for 10 or 15 minutes. For flow cytometric analysis, KikGR-green and KikGR-red were detected with 488nm and 561nm laser excitation and 515–545nm and 574–590 emission filters, respectively, on an LSRII (BD).

Whole-Exome and Sanger Sequencing

Whole exome sequencing was performed by Omega Bioservices using Agilent exome capture and a HiSeq2000 sequencer (Illumina) with 5μg of gDNA prepared from B6.SJL/NCI mouse tissue. Sequence reads were aligned to the C57BL/6 reference sequence and annotated by Omega Bioservices. Nucleotide positions are based on the NCBI m37 assembly. Sanger sequencing (Taqgen) of PCR amplified gDNA was performed using primers listed in Supplementary Table 3 to assay for the presence of coding variants identified by whole exome sequencing in various mouse strains. Based on 27 informative F_2 mice (54 meioses) and 95 F_1xB6.SJL/NCI mice (95 meioses), we estimated the causative mutation in B6.SJL/NCI mice to be within roughly 2 cM (3/149) of *Ptprc*. A list of genes located within 3 cM of *Ptprc* was generated using the linkage map builder tool (http://www.informatics.jax.org/searches/linkmap_form.shtml) from the Mouse Genome Database (MGD, http://www.informatics.jax.org/, 11/2012). Of the 86 coding variants located within 3cM of *Ptprc*, 77 were ruled out as they were reported in the NIH dbSNP database (http://www.ncbi.nlm.nih.gov/snp) or Sanger mouse genomes project (http://www.sanger.ac.uk/cgi-bin/modelorgs/mousegenomes/snps.pl) in A/J, DBA2, FVB.N, NOD or PWD strains, which have Vγ4^{+}CCR6^{+} γδT17 cells (Supplementary Fig. 3a,b, Supplementary Table 1); 1 *Ptprc* variant present in *Ptprc*^{a} (CD45.1) alleles was ruled out[50] (Supplementary Table 1); 6 variants were ruled out based on their presence in B6.SJL/Jax mice by Sanger sequencing; 1 *Cfhr2* coding variant was not confirmed in B6.SJL/NCI mice by Sanger sequencing and

excluded (Supplementary Table 2). The single coding variant remaining was a frameshift mutation in *Sox13* (Supplementary Table 2, Fig. 3a,b).

Statistical analysis

All statistical analysis was performed using Prism software (GraphPad). Ear thickness changes were compared using the 2-way ANOVA test (Fig. 6a). The two-tailed, unpaired t-test was used to compare Sox13 mRNA abundance (Fig. 3c) and γδ T cell frequencies (Supplementary Fig. 3b). The Mann-Whitney U-test was used to compare all other datasets.

Supplementary Material

Refer to Web version on PubMed Central for supplementary material.

ACKNOWLEDGEMENTS

We thank A–K Hadjantonakis and S. Nowotschin for making KikGR mice available, A. Weiss and K. Skrzypczynska for *Ptprc*$^{-/-}$ mice, L. Coussens for FVB/N mice, Q. Tang and A. Mahne for NOD mice, A. Reboldi and Y. Han for helpful discussion, and J. An for expert technical assistance. F.R.V. is supported by NIH T32 AR007175 and a Dermatology Foundation Dermatologist Investigator Research Fellowship Award. Z.W. and K.E.K are supported by Biomedical Research Council Grant 06/1/22/19/469. J.G.C. is an Investigator of the Howard Hughes Medical Institute. This work was supported in part by NIH grant AI045073.

REFERENCES

1. Price AE, Reinhardt RL, Liang HE, Locksley RM. Marking and quantifying IL-17A-producing cells in vivo. PLoS One. 2012; 7:e39750. [PubMed: 22768117]
2. Sutton CE, et al. Interleukin-1 and IL-23 induce innate IL-17 production from gammadelta T cells, amplifying Th17 responses and autoimmunity. Immunity. 2009; 31:331–341. [PubMed: 19682929]
3. Roark CL, et al. Exacerbation of collagen-induced arthritis by oligoclonal, IL-17-producing gamma delta T cells. J Immunol. 2007; 179:5576–5583. [PubMed: 17911645]
4. Cai Y, et al. Pivotal role of dermal IL-17-producing gammadelta T cells in skin inflammation. Immunity. 2011; 35:596–610. [PubMed: 21982596]
5. Mabuchi T, Takekoshi T, Hwang ST. Epidermal CCR6+ gammadelta T cells are major producers of IL-22 and IL-17 in a murine model of psoriasiform dermatitis. J Immunol. 2011; 187:5026–5031. [PubMed: 21984702]
6. Pantelyushin S, et al. Rorgammat+ innate lymphocytes and gammadelta T cells initiate psoriasiform plaque formation in mice. J Clin Invest. 2012; 122:2252–2256. [PubMed: 22546855]
7. Shibata K, Yamada H, Hara H, Kishihara K, Yoshikai Y. Resident Vdelta1+ gammadelta T cells control early infiltration of neutrophils after Escherichia coli infection via IL-17 production. J Immunol. 2007; 178:4466–4472. [PubMed: 17372004]
8. Cho JS, et al. IL-17 is essential for host defense against cutaneous Staphylococcus aureus infection in mice. J Clin Invest. 2010; 120:1762–1773. [PubMed: 20364087]
9. Martin B, Hirota K, Cua DJ, Stockinger B, Veldhoen M. Interleukin-17-producing gammadelta T cells selectively expand in response to pathogen products and environmental signals. Immunity. 2009; 31:321–330. [PubMed: 19682928]
10. Heilig JS, Tonegawa S. Diversity of murine gamma genes and expression in fetal and adult T lymphocytes. Nature. 1986; 322:836–840. [PubMed: 2943999]
11. Havran WL, Allison JP. Developmentally ordered appearance of thymocytes expressing different T-cell antigen receptors. Nature. 1988; 335:443–445. [PubMed: 2458531]
12. Ito K, et al. Different gamma delta T-cell receptors are expressed on thymocytes at different stages of development. Proc Natl Acad Sci U S A. 1989; 86:631–635. [PubMed: 2463632]

13. Kisielow J, Kopf M, Karjalainen K. SCART scavenger receptors identify a novel subset of adult gammadelta T cells. J Immunol. 2008; 181:1710–1716. [PubMed: 18641307]
14. Haas JD, et al. Development of Interleukin-17-Producing gammadelta T Cells Is Restricted to a Functional Embryonic Wave. Immunity. 2012; 37:48–59. [PubMed: 22770884]
15. Melichar HJ, et al. Regulation of gammadelta versus alphabeta T lymphocyte differentiation by the transcription factor SOX13. Science. 2007; 315:230–233. [PubMed: 17218525]
16. Turchinovich G, Hayday AC. Skint-1 identifies a common molecular mechanism for the development of interferon-gamma-secreting versus Interleukin-17-secreting gammadelta T cells. Immunity. 2011; 35:59–68. [PubMed: 21737317]
17. Narayan K, et al. Intrathymic programming of effector fates in three molecularly distinct gammadelta T cell subtypes. Nat Immunol. 2012; 13:511–518. [PubMed: 22473038]
18. Haas JD, et al. CCR6 and NK1.1 distinguish between IL-17A and IFN-gamma-producing gammadelta effector T cells. Eur J Immunol. 2009; 39:3488–3497. [PubMed: 19830744]
19. Gray EE, Suzuki K, Cyster JG. Cutting edge: Identification of a motile IL-17-producing gammadelta T cell population in the dermis. J Immunol. 2011; 186:6091–6095. [PubMed: 21536803]
20. Gray EE, Friend S, Suzuki K, Phan TG, Cyster JG. Subcapsular sinus macrophage fragmentation and CD169+ bleb acquisition by closely associated IL-17-committed innate-like lymphocytes. PLoS One. 2012; 7:e38258. [PubMed: 22675532]
21. Shen FW, et al. Cloning of Ly-5 cDNA. Proc Natl Acad Sci U S A. 1985; 82:7360–7363. [PubMed: 3864163]
22. Kido S, et al. Cloning and characterization of mouse mSox13 cDNA. Gene. 1998; 208:201–206. [PubMed: 9524265]
23. Roose J, et al. The Sox-13 gene: structure, promoter characterization, and chromosomal localization. Genomics. 1999; 57:301–305. [PubMed: 10198172]
24. Brogna S, Wen J. Nonsense-mediated mRNA decay (NMD) mechanisms. Nat Struct Mol Biol. 2009; 16:107–113. [PubMed: 19190664]
25. Sumaria N, et al. Cutaneous immunosurveillance by self-renewing dermal {gamma}{delta} T cells. J Exp Med. 2011; 208:505–518. [PubMed: 21339323]
26. Shibata K, et al. Identification of CD25+ gamma delta T cells as fetal thymus-derived naturally occurring IL-17 producers. J Immunol. 2008; 181:5940–5947. [PubMed: 18941182]
27. Michel ML, et al. Interleukin 7 (IL-7) selectively promotes mouse and human IL-17-producing gammadelta cells. Proc Natl Acad Sci U S A. 2012
28. van der Fits L, et al. Imiquimod-induced psoriasis-like skin inflammation in mice is mediated via the IL-23/IL-17 axis. J Immunol. 2009; 182:5836–5845. [PubMed: 19380832]
29. Nowotschin S, Hadjantonakis AK. Use of KikGR a photoconvertible green-to-red fluorescent protein for cell labeling and lineage analysis in ES cells and mouse embryos. BMC Dev Biol. 2009; 9:49. [PubMed: 19740427]
30. Tomura M, et al. Activated regulatory T cells are the major T cell type emigrating from the skin during a cutaneous immune response in mice. J Clin Invest. 2010; 120:883–893. [PubMed: 20179354]
31. Bromley SK, Yan S, Tomura M, Kanagawa O, Luster AD. Recirculating Memory T Cells Are a Unique Subset of CD4+ T Cells with a Distinct Phenotype and Migratory Pattern. J Immunol. 2012
32. Tomura M, et al. Monitoring cellular movement in vivo with photoconvertible fluorescence protein "Kaede" transgenic mice. Proc Natl Acad Sci U S A. 2008; 105:10871–10876. [PubMed: 18663225]
33. Sallusto F, et al. Switch in chemokine receptor expression upon TCR stimulation reveals novel homing potential for recently activated T cells. Eur J Immunol. 1999; 29:2037–2045. [PubMed: 10382767]
34. Kreslavsky T, Garbe AI, Krueger A, von Boehmer H. T cell receptor-instructed alphabeta versus gammadelta lineage commitment revealed by single-cell analysis. J Exp Med. 2008; 205:1173–1186. [PubMed: 18443226]

35. Lauritsen JP, et al. Marked induction of the helix-loop-helix protein Id3 promotes the gammadelta T cell fate and renders their functional maturation Notch independent. Immunity. 2009; 31:565–575. [PubMed: 19833086]
36. Verbeek S, et al. An HMG-box-containing T-cell factor required for thymocyte differentiation. Nature. 1995; 374:70–74. [PubMed: 7870176]
37. Yu Q, Sharma A, Ghosh A, Sen JM. T cell factor-1 negatively regulates expression of IL-17 family of cytokines and protects mice from experimental autoimmune encephalomyelitis. J Immunol. 2011; 186:3946–3952. [PubMed: 21339363]
38. Ma J, Wang R, Fang X, Ding Y, Sun Z. Critical role of TCF-1 in repression of the IL-17 gene. PLoS One. 2011; 6:e24768. [PubMed: 21935461]
39. Do JS, et al. Cutting edge: spontaneous development of IL-17-producing gamma delta T cells in the thymus occurs via a TGF-beta 1-dependent mechanism. J Immunol. 2010; 184:1675–1679. [PubMed: 20061408]
40. Van Rhijn I, et al. Massive, sustained gammadelta T cell migration from the bovine skin in vivo. J Leukoc Biol. 2007; 81:968–973. [PubMed: 17234682]
41. Hedrick MN, et al. CCR6 is required for IL-23-induced psoriasis-like inflammation in mice. J Clin Invest. 2009; 119:2317–2329. [PubMed: 19662682]
42. von Andrian UH, Mempel TR. Homing and cellular traffic in lymph nodes. Nat Rev Immunol. 2003; 3:867–878. [PubMed: 14668803]
43. Wohler JE, Smith SS, Zinn KR, Bullard DC, Barnum SR. Gammadelta T cells in EAE: early trafficking events and cytokine requirements. Eur J Immunol. 2009; 39:1516–1526. [PubMed: 19384874]
44. Gilliet M, et al. Psoriasis triggered by toll-like receptor 7 agonist imiquimod in the presence of dermal plasmacytoid dendritic cell precursors. Arch Dermatol. 2004; 140:1490–1495. [PubMed: 15611427]
45. Laggner U, et al. Identification of a novel proinflammatory human skin-homing Vgamma9Vdelta2 T cell subset with a potential role in psoriasis. J Immunol. 2011; 187:2783–2793. [PubMed: 21813772]
46. Kishihara K, et al. Normal B lymphocyte development but impaired T cell maturation in CD45-exon6 protein tyrosine phosphatase-deficient mice. Cell. 1993; 74:143–156. [PubMed: 8334701]
47. Phan TG, Green JA, Gray EE, Xu Y, Cyster JG. Immune complex relay by subcapsular sinus macrophages and noncognate B cells drives antibody affinity maturation. Nat Immunol. 2009; 10:786–793. [PubMed: 19503106]
48. Tortola L, et al. Psoriasiform dermatitis is driven by IL-36-mediated DC-keratinocyte crosstalk. J Clin Invest. 2012
49. Matloubian M, et al. Lymphocyte egress from thymus and peripheral lymphoid organs is dependent on S1P receptor 1. Nature. 2004; 427:355–360. [PubMed: 14737169]
50. Zebedee SL, Barritt DS, Raschke WC. Comparison of mouse Ly5a and Ly5b leucocyte common antigen alleles. Dev Immunol. 1991; 1:243–254. [PubMed: 1822988]

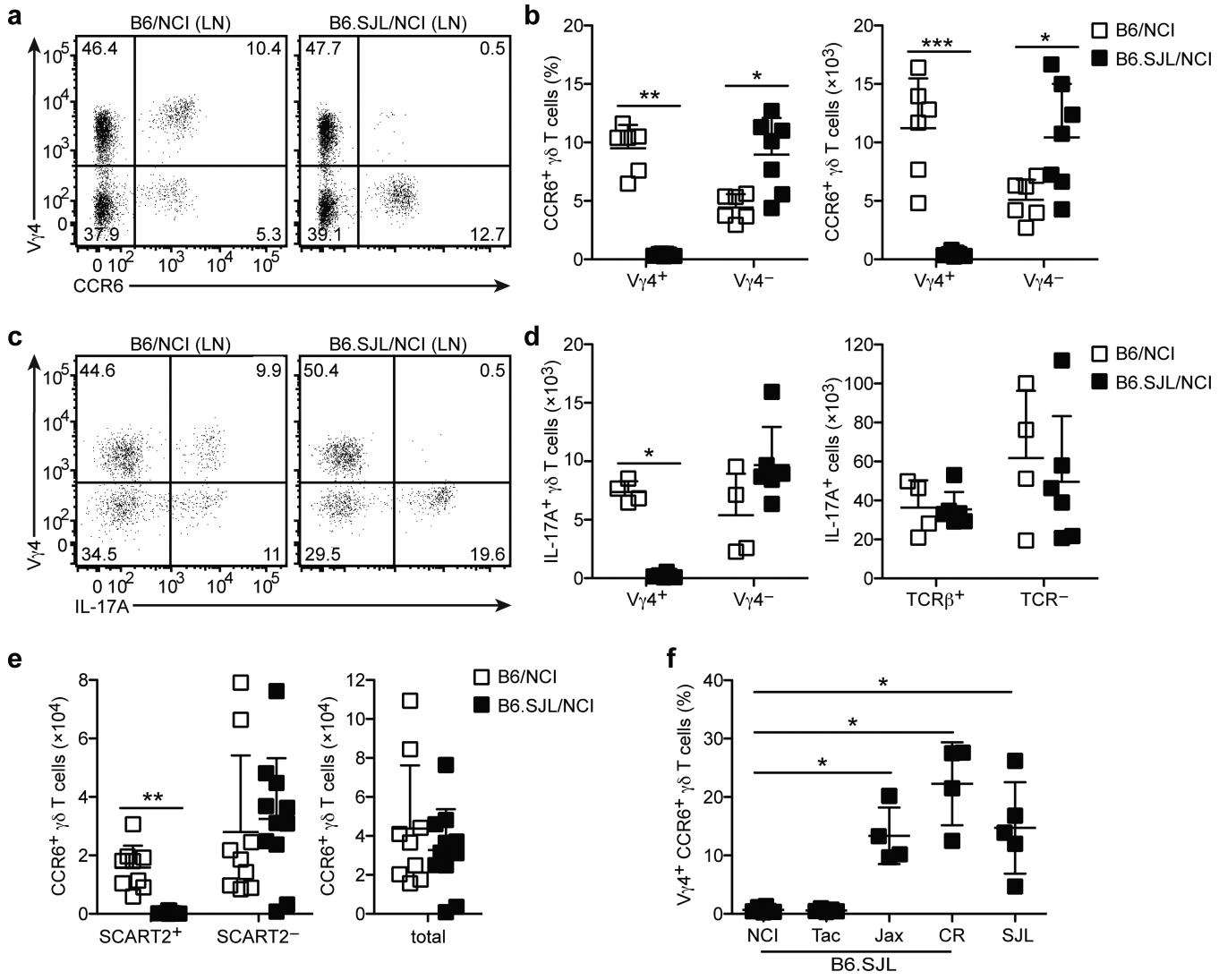

Figure 1. B6.SJL/NCI and B6.SJL/Tac mice lack Vγ4$^+$ γδT17 cells

(**a**) Flow cytometric detection of Vγ4$^+$CCR6$^+$ γδ T cells in digested LN cell suspensions from B6/NCI and B6.SJL/NCI mice, gated on total γδ T cells. (**b**) Quantification of LN CCR6$^+$ Vγ4$^+$ and Vγ4$^-$ γδ T cell frequency (plotted as % of total γδ T cells) and absolute number in B6/NCI and B6.SJL/NCI mice gated as in (**a**). (**c**) Intracellular IL-17A staining of digested LN cell suspensions from B6/NCI and B6.SJL/NCI mice following PMA+I stimulation, gated on total γδ T cells. (**d**) Quantification of the absolute number of LN IL-17$^+$ Vγ4$^+$ and Vγ4$^-$ γδ T cells (left panel) and IL-17$^+$ αβ T cells and TCR$^-$ cells (right panel) in B6/NCI and B6.SJL/NCI mice. (**e**) Quantification of the absolute number of SCART2$^+$, SCART2$^-$, and total CCR6$^+$ γδ T cells in ear skin dermal cell suspensions from B6/NCI and B6.SJL/NCI mice. (**f**) Quantification of LN Vγ4$^+$CCR6$^+$ γδ T cell frequency in B6.SJL and SJL mice from various vendors gated as in (**a**), plotted as % of total γδ T cells. Each symbol represents an individual mouse; horizontal and vertical bars represent the mean (± s.d.) (**b,d–f**). *P≤0.01, **P≤0.005, ***P≤0.001. Data are representative of three

experiments with 6–7 mice (**a,b**), three experiments with 4–6 mice (**c,d**), five experiments with 9–11 mice (**e**), and at least two experiments with 4 mice for each strain (**f**).

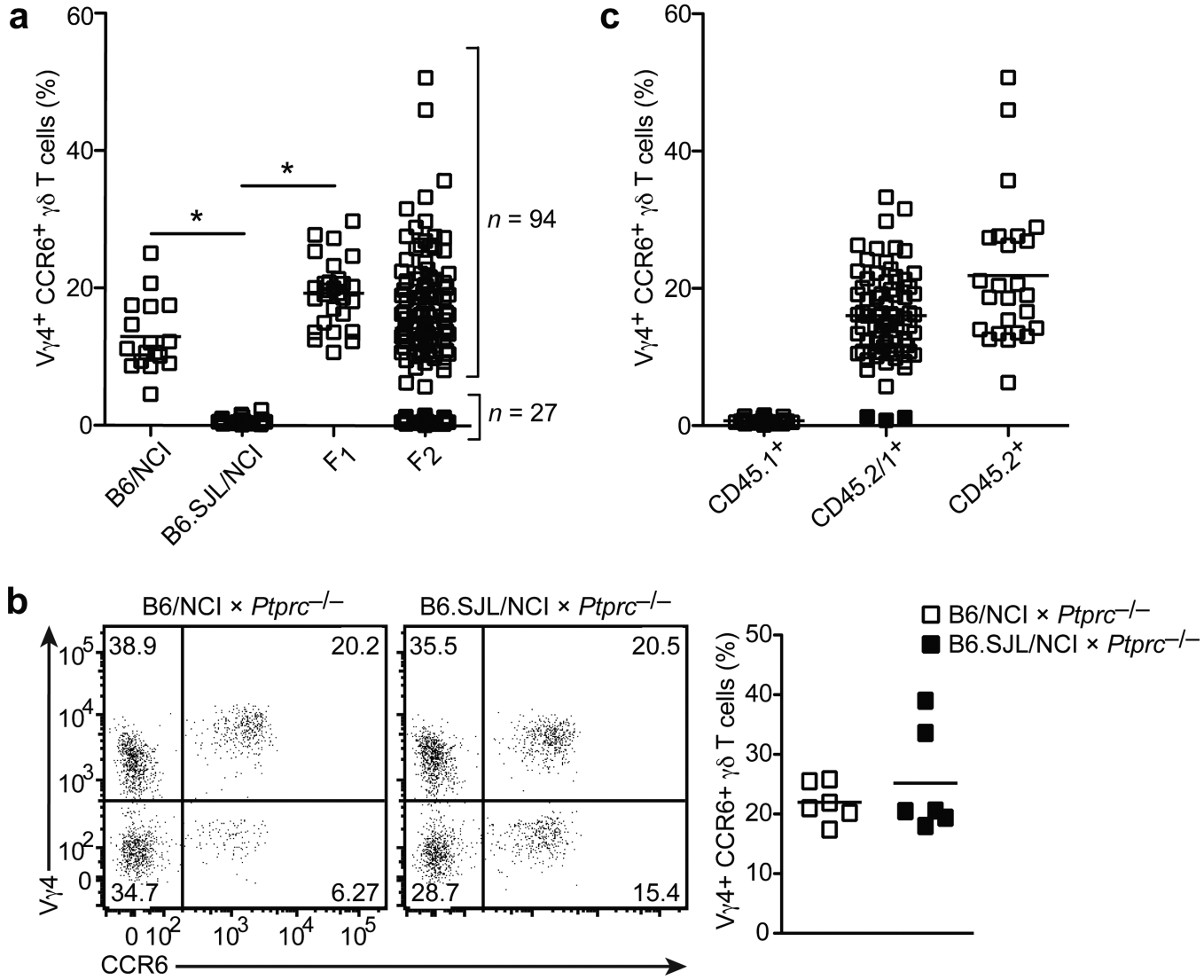

Figure 2. Vγ4$^+$ γδT17 cell deficiency is an autosomal, recessive trait controlled by a single locus

(**a**) Quantification of LN Vγ4$^+$CCR6$^+$ γδ T cell frequency (plotted as % of total γδ T cells) in mice of the indicated type. (**b**) Flow cytometric detection of Vγ4$^+$CCR6$^+$ γδ T cells in digested lymph node cell suspensions from B6/NCI and B6.SJL/NCI × *Ptprc*$^{-/-}$ mice (3 to 6 weeks of age), gated on total γδ T cells (left panel); quantification of LN Vγ4$^+$CCR6$^+$ γδ T cell frequency (plotted as % of total γδ T cells) in mice of the indicated type (right panel). (**c**) Quantification of LN Vγ4$^+$CCR6$^+$ γδ T cell frequency (plotted as % of total γδ T cells) in F_2 mice that are CD45.1$^+$, CD45.1$^+$/2$^+$, and CD45.2$^+$. The three recombination events are indicated by the filled squares. Each symbol represents an individual mouse; horizontal bars represent the mean (**a–c**). *P≤0.0001. Data are representative of 18 experiments with at least 15 mice of each type (**a,c**) and two experiments with 6 mice (**b**).

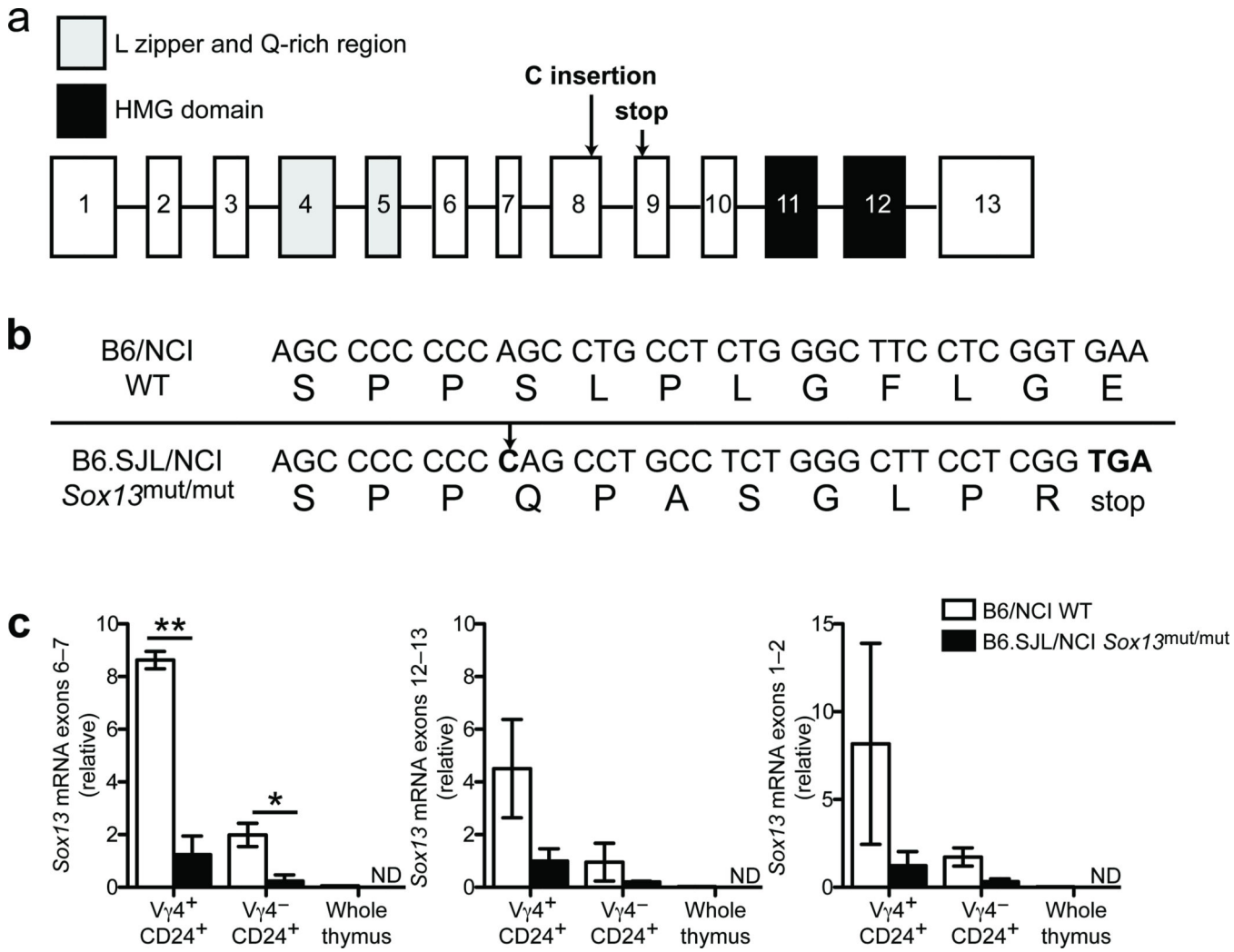

Figure 3. B6.SJL/NCI and B6.SJL/Tac mice harbor a frameshift mutation in *Sox13*

(**a**) Schematic of the *Sox13* gene; exons are indicated in squares and introns by lines (not drawn to scale). The C nucleotide insertion and premature stop codon are indicated with arrows. (**b**) *Sox13* cDNA and amino acid sequence in wild-type (WT, B6/NCI) and *Sox13*$^{mut/mut}$ (B6.SJL/NCI) mice. The C nucleotide insertion is indicated with an arrow. (**c**) Quantification of *Sox13* mRNA in sorted V$\gamma4^+$CD24$^+$ and V$\gamma4^-$CD24$^+$ $\gamma\delta$ T cells from adult thymi of WT (B6/NCI) and *Sox13*$^{mut/mut}$ (B6.SJL/NCI) mice, and whole thymus from a WT (B6/NCI) mouse. Real-time PCR data are shown for primer pairs spanning *Sox13* exons 6–7 (left), exons 12–13 (center) and exons 1–2 (right). Horizontal and vertical bars represent the mean (± s.d.). *$P \leq 0.05$, **$P \leq 0.01$. Data are representative of two experiments (sorted $\gamma\delta$ T cells) or one experiment (whole thymus).

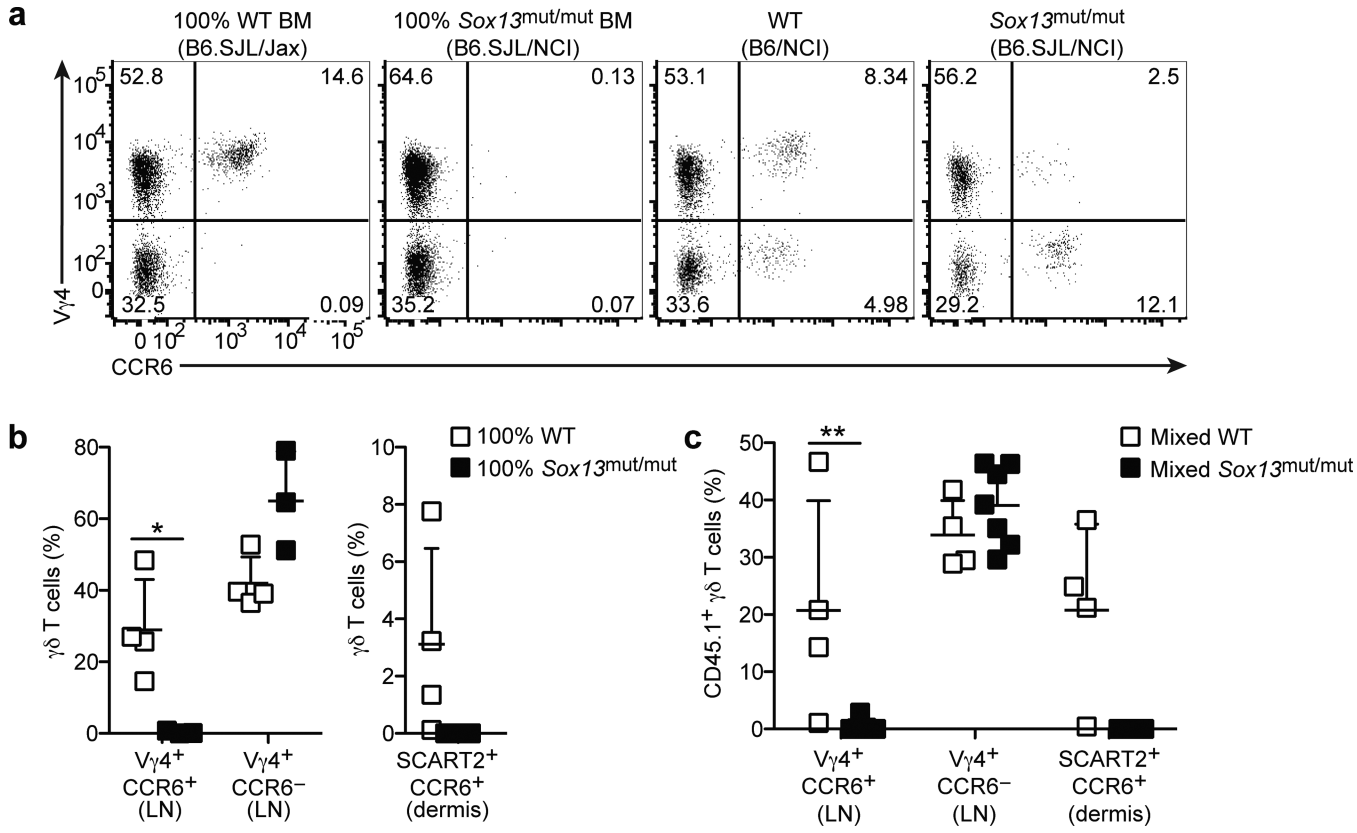

Figure 4. Sox13 intrinsically regulates development of Vγ4$^+$ γδT17 cells

(a) Flow cytometric detection of Vγ4$^+$CCR6$^+$ γδ T cells in digested LN cell suspensions from irradiated CD45.2$^+$ *TCR*δ$^{-/-}$ mice reconstituted with BM from CD45.1$^+$ WT (B6.SJL/Jax) or *Sox13*$^{mut/mut}$ (B6.SJL/NCI) mice and non-chimeric WT (B6/NCI) and *Sox13*$^{mut/mut}$ (B6.SJL/NCI) mice, gated on total γδ T cells. **(b)** Quantification of LN Vγ4$^+$CCR6$^+$ and Vγ4$^+$CCR6$^-$ γδ T cell frequency (plotted as % of total γδ T cells, left panel) and dermal SCART2$^+$CCR6$^+$ γδ T cells (plotted as % of CD45.1$^+$ dermal cells, right panel) in CD45.2$^+$ *TCR*δ$^{-/-}$ mice reconstituted with BM of the indicated type. **(c)** Quantification of CD45.1$^+$ LN Vγ4$^+$CCR6$^+$ and Vγ4$^+$CCR6$^-$ and dermal SCART2$^+$CCR6$^+$ γδ T cells (plotted as % of indicated γδ T cell subset expressing CD45.1) in CD45.2$^+$ *TCR*δ$^{-/-}$ mice reconstituted with a mixture of BM from CD45.2$^+$ WT (B6/NCI) and CD45.1$^+$ WT (B6.SJL/Jax) or *Sox13*$^{mut/mut}$ (B6.SJL/NCI) mice. Each symbol represents an individual mouse; horizontal and vertical bars represent the mean (± s.d.). **P*≤0.1, ***P*≤0.01. Data are representative of three experiments with 3–7 mice.

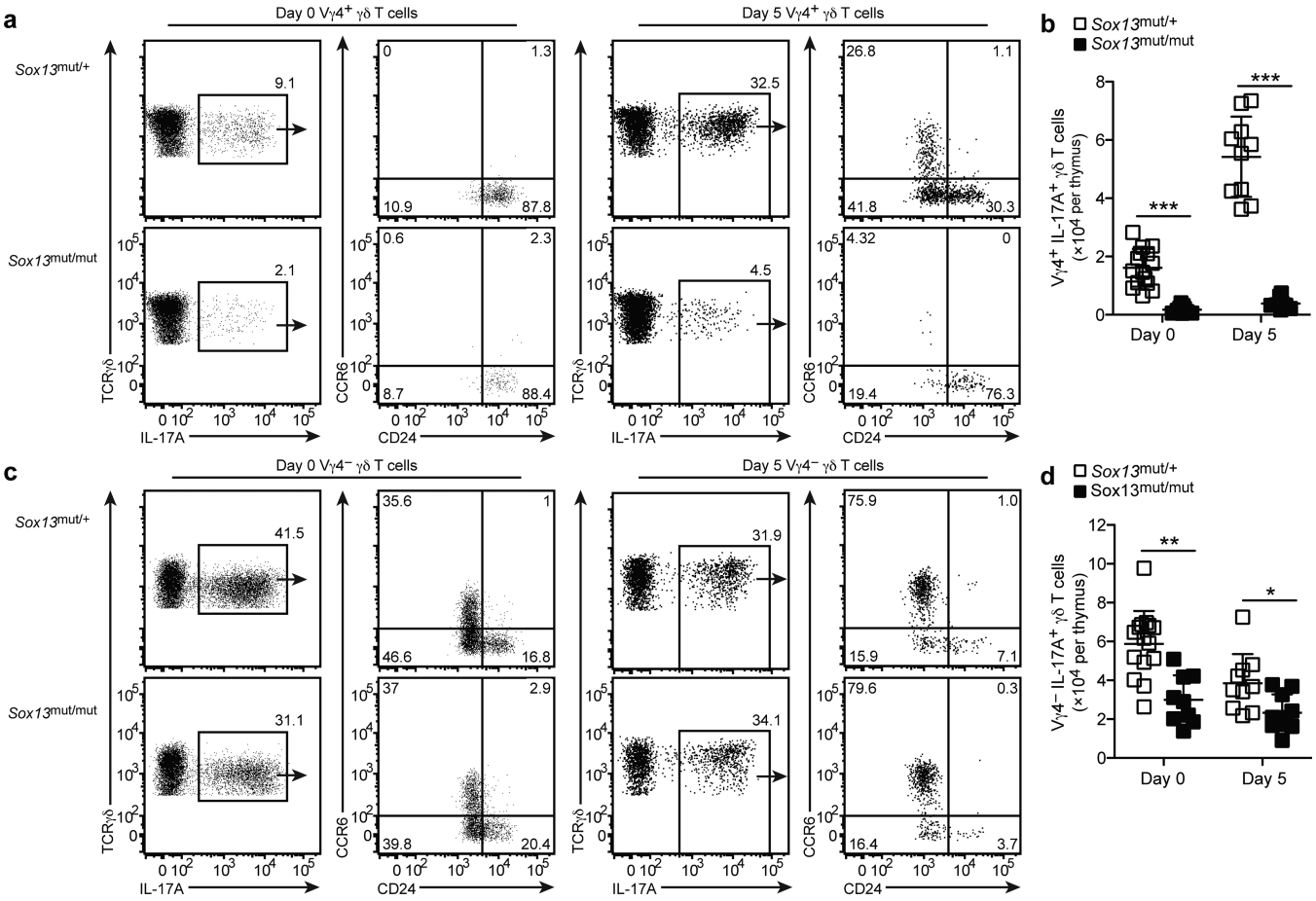

Figure 5. Vγ4$^+$ γδT17 development is blocked in the neonatal thymus in *Sox13*$^{mut/mut}$ mice

F_1 mice were backcrossed to *Sox13*$^{mut/mut}$ (B6.SJL/NCI) mice to generate *Sox13*$^{mut/+}$ or *Sox13*$^{mut/mut}$ neonates. (**a,c**) Intracellular IL-17A staining of thymocytes from day 0 and 5 neonates of the indicated type following stimulation with PMA+I, gated on Vγ4$^+$ (**a**) or Vγ4$^-$ (**c**) γδ T cells. (**b,d**) Quantification of Vγ4$^+$ (**b**) or Vγ4$^-$ (**d**) IL-17A$^+$ γδ T cells from day 0 and 5 neonatal thymi of the indicated type. Each symbol represents an individual mouse, horizontal and vertical bars represent the mean (± s.d.). **P*≤0.01, ***P*≤0.001, ****P*≤0.0001. Data are representative three experiments with at least 9 mice.

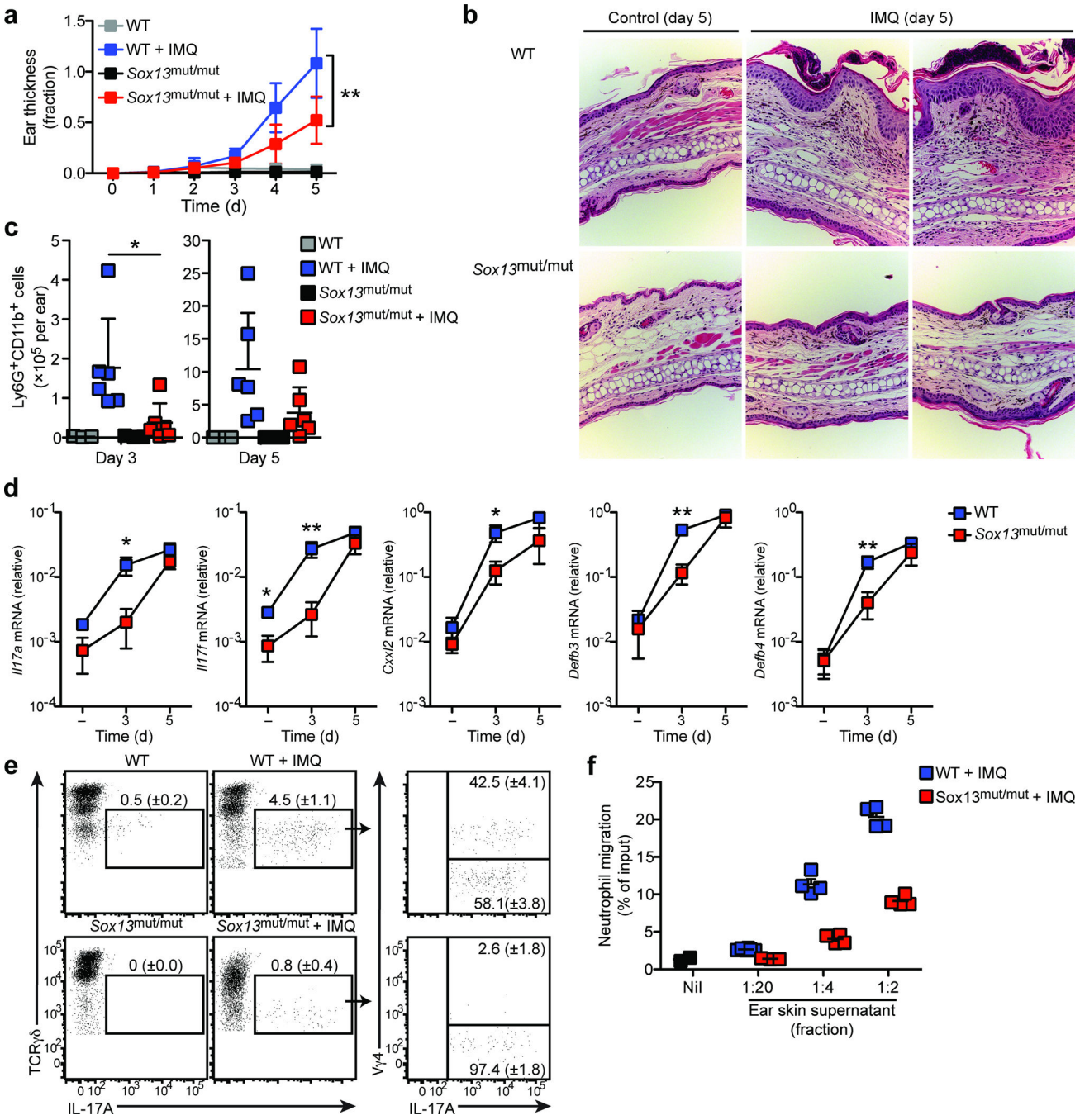

Figure 6. *Sox13*$^{mut/mut}$ (B6.SJL/NCI) mice are protected from psoriasis-like dermatitis

(**a**) Quantification of ear skin thickness, plotted as fraction increase relative to baseline (day 0), of WT (B6/NCI) and *Sox13*$^{mut/mut}$ (B6.SJL/NCI) mice treated with imiquimod or control cream daily for 5 days. Boxes represent the mean (± s.d.). (**b**) H&E staining of ear skin from WT and *Sox13*$^{mut/mut}$ mice treated per (**a**) for 5 days. (**c**) Quantification of Ly6G^{+}CD11b^{+} neutrophils in ear skin cell suspensions from WT and *Sox13*$^{mut/mut}$ mice treated per (**a**) for 3 or 5 days. Each symbol represents an individual mouse; horizontal bars represent the mean (± s.d.). (**d**) RT-PCR quantification of ear skin mRNA from WT and *Sox13*$^{mut/mut}$ mice

treated with control (−) or imiquimod cream for 3 or 5 days. Boxes represent the mean (± s.d.). (**e**) Intracellular IL-17A staining of ear skin cell suspensions from WT and *Sox13*$^{mut/mut}$ mice treated as in (**a**) for 3 days and digested in the presence of Brefeldin A, gated on total γδ T cells. Mean (± s.d.) is indicated. (**f**) Transwell assay of neutrophil migration to ear skin supernatants prepared from WT and *Sox13*$^{mut/mut}$ mice treated as in (**a**) for 3 days. Each symbol represents migration from an individual transwell, horizontal bars represent the mean (± s.d.). **P*≤0.05, ***P*≤0.01. Data are representative of three experiments with 3–6 mice (**a–d**), two experiments with 2–5 mice (**e**), and four experiments with 9 mice (**f**).

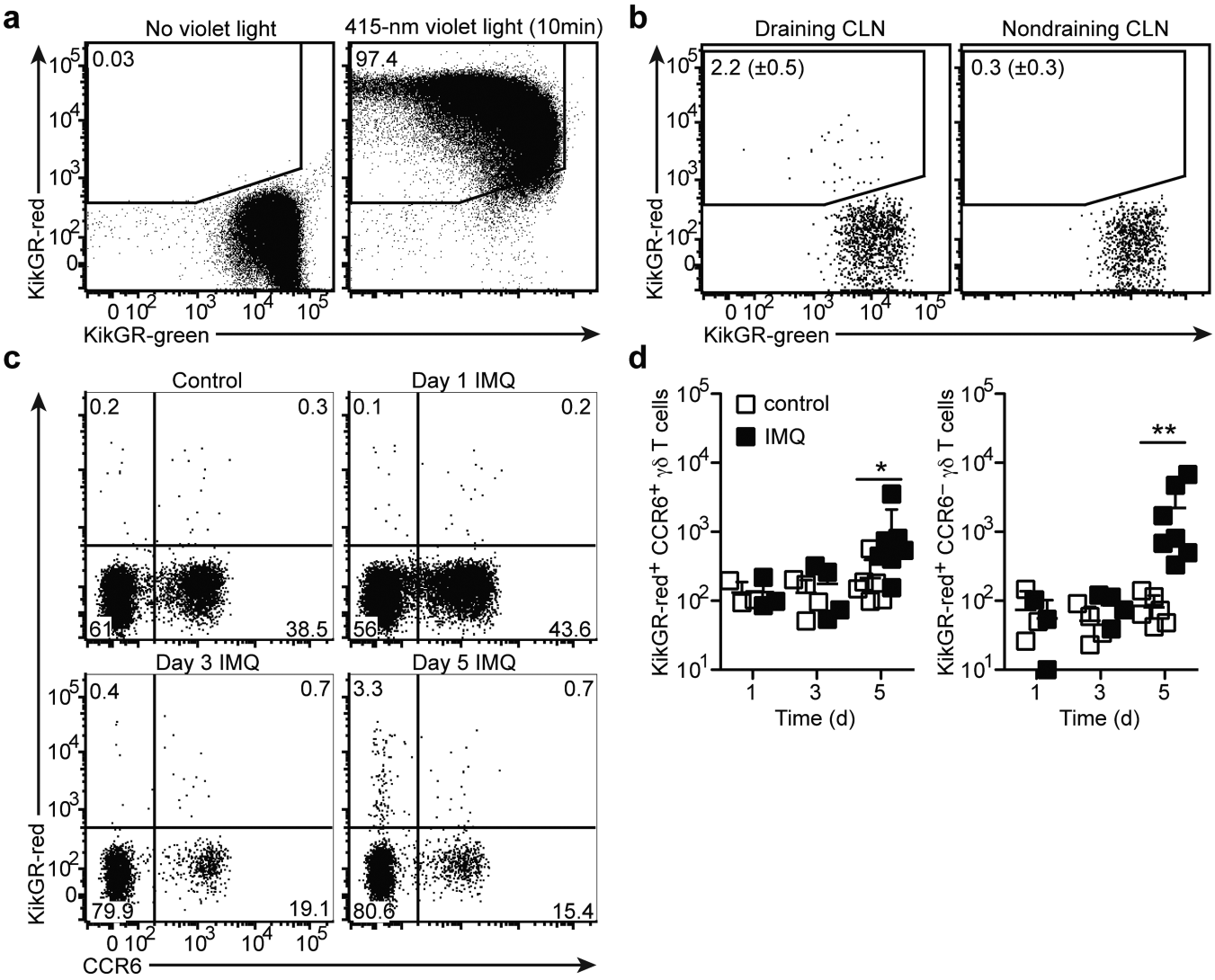

Figure 7. γδT17 cells migrate from skin to draining lymph nodes at low rates

(**a**) Flow cytometric detection of KikGR-red$^+$ and KikGR-green$^+$ cells in ear skin cell suspensions harvested immediately after exposure to violet light (right) or untreated (left), gated on total live cells. (**b**) Flow cytometric detection of KikGR-red$^+$ CCR6$^+$ γδ T cells in draining (left) and non-draining (right) cervical LNs (CLN) harvested 24 hours after ear skin photoconversion, gated on total CCR6$^+$ γδ T cells. The mean (± s.d.) %KikGR-red$^+$ cells from four independent experiments are indicated (n=4 mice). (**c**) Flow cytometric detection of KikGR-red$^+$ CCR6$^+$ and CCR6$^-$ γδT cells in draining CLNs of control and imiquimod-treated ear skin harvested at the indicated day of imiquimod treatment and one day after photoconversion, gated on total γδ T cells. (**d**) Quantification of KikGR-red$^+$ CCR6$^+$ and CCR6$^-$ γδ T cells in draining CLNs of control (empty squares) and imiquimod-treated (filled squares) ear skin, treated as in (**c**). Each symbol represents an individual CLN; horizontal bars represent the mean (± s.d.). *P≤0.05, **P≤0.001. Data are representative three experiments with 3 mice (**a**), four experiments with 4 mice (**b**), and 6 experiments with 3–7 mice at each time point (**c,d**).

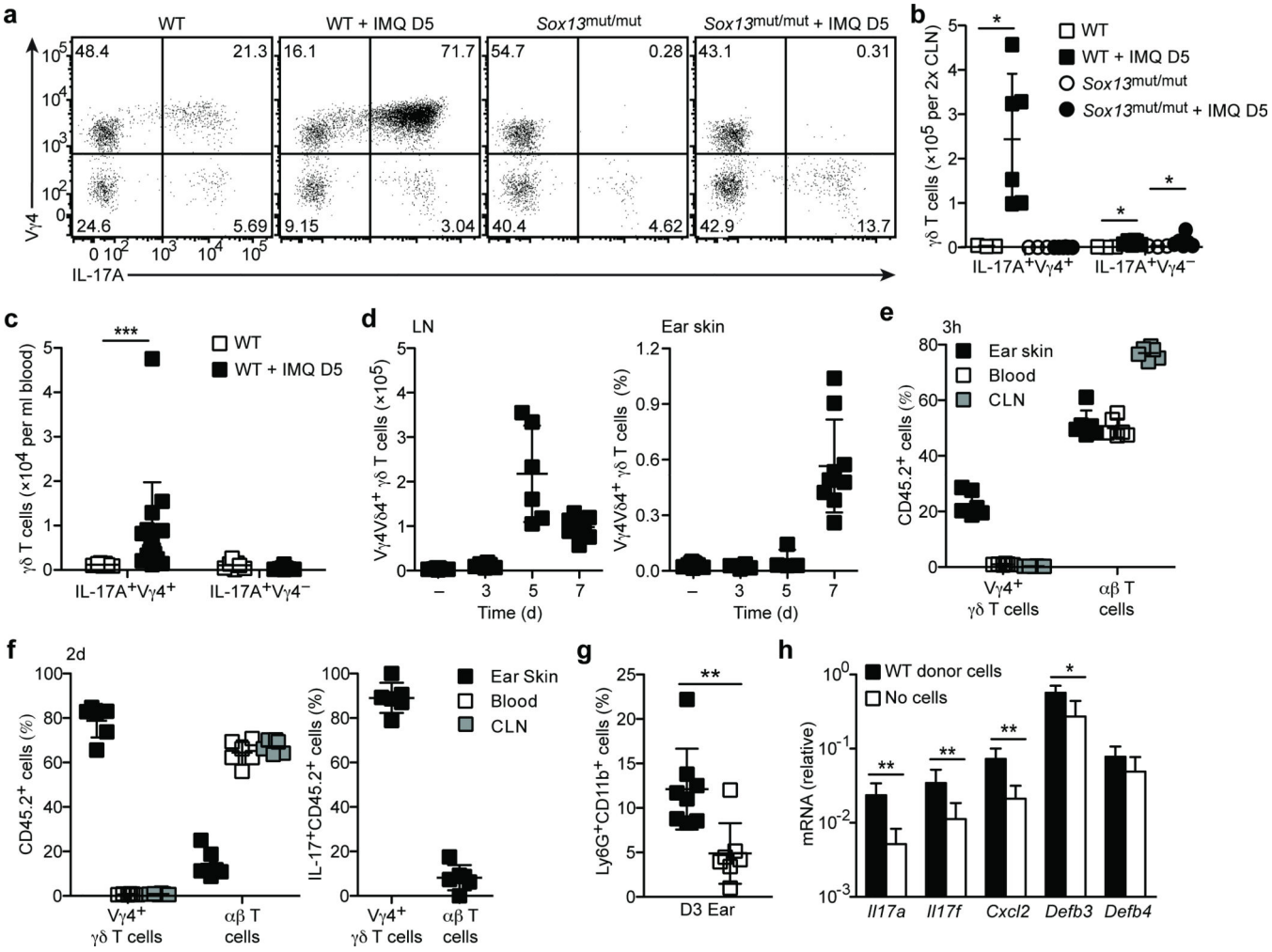

Figure 8. Vγ4$^+$ γδT17 cells expand in draining LNs and home to inflamed ear skin

(**a**) Intracellular IL-17A staining of PMA+I stimulated CLN cell suspensions from WT (B6/NCI) and *Sox13*$^{mut/mut}$ (B6.SJL/NCI) mice treated with imiquimod or control cream for 5 days, gated on total γδ T cells. (**b,c**) Quantification of IL-17A$^+$ γδ T cells in CLNs (**b**) and blood (**c**) from mice treated as in (**a**). (**d**) Quantification Vγ4$^+$Vδ4$^+$ γδ T cell number in CLNs (left panel) or frequency in ear skin (right panel, plotted as % of live cells) treated as in (**a**) for 3–7 days. (**e**) Quantification of donor T cells in the indicated tissues, plotted as percent of CD45.2$^+$ donor cells, from day 2 imiquimod-treated *Sox13*$^{mut/mut}$ recipients 3 hours after transfer of CLN cells from day 5 or 7 imiquimod-treated WT mice. (**f**) Quantification of donor T cells in the indicated tissues, plotted as percent of CD45.2$^+$ (left panel) and IL-17A$^+$CD45.2+ (right panel) donor cells from day 3 imiquimod-treated *Sox13*$^{mut/mut}$ recipients 2 days after transfer of CLN cells from day 5 imiquimod-treated WT mice. (**g,h**) Quantification of Ly6G$^+$CD11b$^+$ neutrophils, plotted as percent of CD45$^+$ cells (**g**), and mRNA by RT-PCR (**h**) in ear skin from mice treated as in (**f**). Each symbol represents an individual mouse; horizontal bars represent the mean (± s.d.). *P≤0.05,

$P \leq 0.01$, ***$P \leq 0.001$. Data are representative of at least three experiments (a–e,g**) or two experiments with at least 5 mice (**f,h**).